Dimeric Structure of the Blue Light Sensor Protein Photozipper in the Active State

[†]Kohei Ozeki, [†]Hiroyuki Tsukuno, [†$]Hiroki Nagashima, [‡*]Osamu Hisatomi and [†*]Hiroyuki Mino

[†]Division of Material Science, Graduate school of Science, Nagoya University, Chikusa-ku, Furo-cho, Nagoya, 464-8602, Japan, [‡]Department of Earth and Space Science, Graduate School of Science, Osaka University, Osaka, 560-0043, Japan

Supporting Information Placeholder

ABSTRACT: The light oxygen voltage-sensing (LOV) domain plays a crucial role in blue light (BL) sensing in plants and microorganisms. LOV domains are usually associated with the effector domains, and regulate the activities of effector domains in a BL-dependent manner. Photozipper (PZ) is monomeric in the dark state. BL induces reversible dimerization of PZ and subsequently increases its affinity for the target DNA sequence. In this study, we report the analyses of PZ by pulsed electron-electron double resonance (PELDOR). The neutral flavin radical was formed by BL illumination in the presence of dithiothreitol in both the LOV-C254S (without the bZIP domain) and the PZ-C254S mutants, where the cysteine residue responsible for adduct formation was replaced with serine. The magnetic dipole interactions of 3 MHz between the neutral radicals were detected in both LOV-C254S and PZ-C254S, indicating that these mutants underwent dimerization in the radical state. The PELDOR simulation showed that the distance between the radical pair is close to that estimated from the dimeric crystal structure in the 'light state' [Heintz, U.; Schlichting, I., *Elife* **2016,** *5*, e11860.], suggesting that in the radical state, LOV domains in PZ-C254S form a dimer similar to that of LOV-C254S, which lacks the bZIP domain. The BL-induced conformational change of PZ probably causes the dimerization of the LOV domain and the coiled-coil formation of the bZIP domain, which contribute to its increased affinity for the target DNA sequence.

As photomorphogenesis is inevitable to optimize the efficiency of photosynthesis, plants have developed light sensor proteins, like the phototropins and phytochromes. Light oxygen voltage-sensing (LOV) domains play crucial roles for the blue light (BL) sensing function of phototropins, and regulate the activity of the kinase domains (effector domains) in a BL-dependent manner. Aureochrome-1 (AUREO1) is composed of a basic leucine zipper (bZIP) domain and a LOV domain, and is suggested to be responsible for the branching response of a stramenopile alga, *Vaucheria frigida*[1, 2]. The bZIP domain is an α-helical DNA-binding motif found in a family of eukaryotic transcription factors that recognizes sequences of 4-10 base pairs in the target DNA[3-7]. AUREO1 recognizes the target DNA sequence of TGACGT[2].

In the initial reactions in the LOV domain, the flavin mononucleotide (FMN) molecule is photo-excited by BL illumination to form a triplet state. The FMN triplet forms an adduct with a highly conserved, nearby cysteine residue, which prompts simultaneous proton transfers from the cysteine to FMN[8-10]. These reactions are also found in aureochromes. In AUREO1, this series of reactions induces the dimerization of the LOV domain, to enhance the affinity for DNA[11-17]. Therefore, dimerization would be the key reaction for aureochromes[11-14].

Although the structure of the aureochrome complex in solution is still unknown, crystal structures of the LOV domains of aureochromes have been reported[15, 18, 19]. Development of the LOV domain of *Vaucheria frigida* AUREO1 in the dark state resulted in three dimers in crystal, and the three dimers with crystal in the light state was obtained by illumination of the crystal. Alternatively, the LOV domain of *Phaeodactylum tricornutum* AUREO1a has been reported to be either one dimer[15] or two dimers[18] in the dark state, and to be dimeric in the crystal grown under light[15]. These structures are inconsistent with each other, which might be due to the flexibility of the protein.

Photozipper (PZ) is a functional protein designed from AUREO1, in which contains two parts: the LOV domain and the bZIP domain[11]. Therefore, PZ is not only a good tool for understanding the function of AUREO1, but also a good candidate for optogenetic module. In this work, we report the radical state of PZ in the active state determined by electron paramagnetic resonance (EPR). Our data suggest that the protonation of FMN induces the dimerization of PZ.

Wild-type expression vectors of PZ and LOV (without the bZIP domain) were mutated with a PrimeSTAR mutagenesis kit (Takara Bio), using PZ-C254S_F (CGTAACTCCCGCTTCCTGCAAGGTCC) and PZ-C254S_R (GAAGCGGGAGTTACGGCCCAGGATCT) primers, and introduced into BL21(DE3) cells (Invitrogen)[11]. Recombinant PZ and LOV mutants (Fig.S1), in which Cys254 was replaced with Ser (C254S), were prepared as described previously[12, 13]. The final concentrations of the samples were 40 μM for continuous wave (CW) EPR and 150-260 μM for pulsed EPR. Samples were suspended in a buffer containing 400 mM NaCl and 20 mM Tris/HCl (pH 7.0). Dithiothreitol (DTT) was added for the radical formation with the 1mM final concentration. For DNA binding, 100 μM double-stranded oligonucleotide (taken form 250 μM stock solution in 100mM NACl, Apo: 5'111-1GCTGTCTGACGTCAGACAGC-3, was added to PZ[13]. Final concentration for DNA binding was 150 μM for PZ and 100 μM for DNA, respectively, in 253 mM NaCl and 11 mM Tris/HCl (pH 7.0)

CW-EPR measurements were carried out with X-band (9.64 GHz) using a Bruker ESP-300E EPR spectrometer (Bruker DE) with a dielectric resonator (ER4117DHQH, Bruker DE). The sample was inserted into a quartz flat cell. Pulsed EPR and pulsed electron-electron double resonance (PELDOR) were carried out with Q-band (34 GHz) using a Bruker E680 with a dielectric resonator (EN 5107D2, Bruker DE) and an Oxford Instruments liquid helium cryostat (CF935P, Oxford UK). The π/2-τ-π sequence was used to measure the ESE field-swept spectra. The pulse lengths were 28 ns for π/2 and 48 ns for π. The time interval τ between the microwave pulses was set to 200 ns.

The π/2-τ1-π-τ1-τ2-π sequence with a time interval τ1 of 200 ns steps was used for four-pulse ELDOR [20, 21] with pumping frequency of 34.01 GHz.

Samples were illuminated with a 408 nm Diode Laser (NDHV220APA, NICHIA; ITC 510, THORLABS) through a 10-

mm diameter glass fiber. The power was set to 40 mW. Absorption spectra were measured using a Hitachi U-3300. The spin density distribution of FMN was calculated using Gaussian09 with the upbepbe/6-311g(d) basis set [22].

Figure 1 shows the absorption spectra of LOV-C254S in the presence of DTT, (a) before and (b) after illumination. The replacement of Cys254 with Ser in the LOV domain prevents formation of the adduct with FMN. The light-induced signal around 500-600 nm shows the formation of the flavin neutral radical $FMNH^{\bullet}$. Figure 2 shows the EPR spectra of LOV-C254S in the presence of DTT. An EPR signal with about 22 G width at g = 2.005 was detected in the presence of DTT. Despite a small amount of accumulation of the free radical, the $FMNH^{\bullet}$ signal did not accumulate in the absence of DTT. Therefore, DTT works as an electron acceptor and proton donor to FMN. A flavin neutral radical is well-characterized as g = 2.0035 with 20 G width[23]. Slight difference might be due to overlapping of the free radical with large modulation depth.

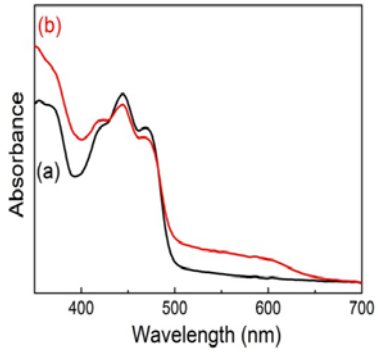

Figure 1: Absorption spectra of LOV-C254S in the presence of dithiothreitol (DTT) (a) before and (b) after illumination for 6 min. The sample concentration was 40 μM.

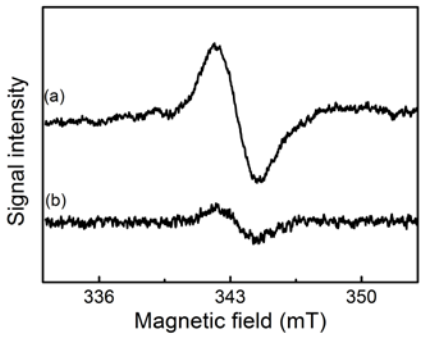

Figure 2. CW EPR spectra of the LOV-C254S domain in the (a) presence and (b) absence of DTT. The samples were measured under BL illumination at room temperature. Spectra of the dark states were subtracted. The sample concentration was 40 μM. Experimental conditions: microwave frequency, 9.64 GHz; microwave power, 1 mW; modulation frequency, 100 kHz; modulation amplitude, 10 G.

Figure 3 shows the (a) PELDOR signal of the $FMNH^{\bullet}$ radical in LOV-C254S in the presence of DTT and (b-f) simulations. The sample was illuminated for 10 min, and subsequently frozen in liquid nitrogen. An oscillation pattern of about 3 MHz was observed. Using the simple point dipole approximation, the distance between the two radicals was estimated as 25.1 Å, which was close to the distance between the two FMN molecules in the crystal structure of the LOV dimer[18]. The results suggest that LOV-C254S is dimeric in the observed condition.

PELDOR is the powerful tool to determine distances between unpaired electrons. The interaction between flavin radicals have been also previously detected[24]. The PELDOR signals for the two flavin radicals on both LOV-C254S and PZ-C254S were observed with a distance of about 25 Å, assuming the point dipole approximation. As the electron spin is actually distributed on the molecule, the spin distribution on the molecules should be considered. Table T1 summarizes the spin density distribution on flavin molecule, where the numbering of the atoms is based on Figure S3. The PELDOR signal amplitude X (τ') as a function of the time interval τ' between the 1st and 2nd pulses was taken as[20, 21]:

$$X(\tau') \propto 1 - p[1 - \cos(2\pi D\tau')] \quad (1)$$

with

$$D = \sum_{i,j} \rho_i \rho_j \frac{g^2\beta^2}{h R_{ij}^3}(1 - 3\cos^2\theta_{ij}) \quad (2)$$

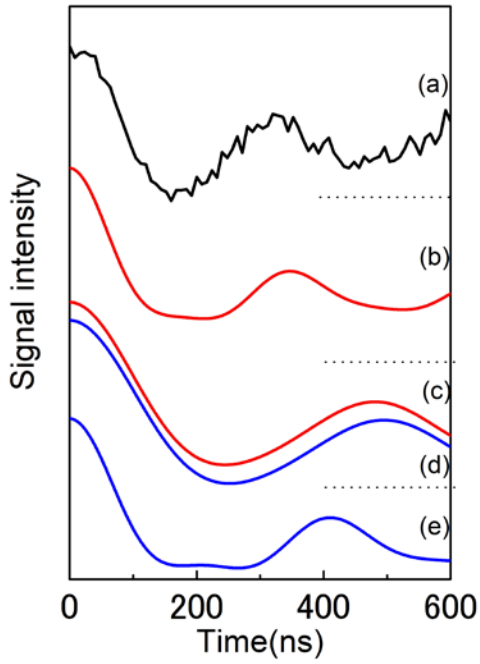

Figure 3: PELDOR signals of LOV-C254S for (a) experiments and (b-f) simulations. Trace a was divided by the background signal as a linear function. Traces c-f were calculated from the spin distribution on flavin and coordinates from the crystal structures of (b) PDB 5dkl, (c) PDB 3ue6, (d) PDB 3ulf and (e) 5a8b [15, 18, 19]. The crystal conditions: (b, d) the light states; (c, e, f) the dark states. The sample concentration was 220 μM. Experimental conditions: microwave frequency, 33.97 GHz for observation and 34.01 GHz for pumping; duration of the mi-

crowave pulses, 24 for π/2 and 48 ns for π; repetition rate, 0.1 kHz; temperature, 40 K.

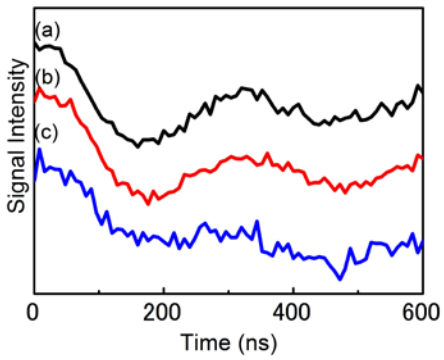

Figure 4: PELDOR signals of (a) LOV-C254S and (b) PZ-C254S without DNA and (c) with DNA. The signals were divided by the background signal as a linear function. The sample concentrations: (a) 220 μM, (b) 260 μM and (c) 150 μM. Experimental conditions were the same as for Figure 3.

where, ρ_i and ρ_j are the spin density at the *i*-th (i = 1-16) carbon/nitrogen/oxygen atom of the radicals 1 and 2, respectively. R_{ij} is the length between the *i*-th and *j*-th carbon/nitrogen/oxygen atom of radicals 1 and 2. Θ_{ij} is the angle between the external magnetic field $\boldsymbol{H}$ and the distance vector $\boldsymbol{R}_{ij}$. The g-factors for the radicals were assumed to be 2. The signal amplitude I(τ′) is given by the surface integration:

$$I(\tau') = \iint X(\tau') \sin\theta \mathrm{d}\theta \mathrm{d}\varphi \qquad (3)$$

We simulated PELDOR signals using the spin density distribution of flavin and the coordinates in the crystal structures.

Figure 3 shows the comparison with the different crystal structures[15, 18, 19]. Traces b-f (Figure 3) are the calculations from the spin distribution on flavin and coordinates from the crystal structures of (b) PDB 5dkl, (c) PDB 3ue6, (d) PDB 3ulf and (e) 5a8b [15, 18, 19]. The 'light state' of the crystal structure in *P. tricornutum*[15] (trace b) shows in good agreement with the experimental signal (trace a), which is consistent with the point that aureochrome functions as a dimeric structure in the light state. Therefore, we concluded that our observed state is close to the 'light state' having the dimeric crystal structure in *P. tricornutum*[15]. Conversely, the other structures do not fit to the experimental result.

The slight difference between traces a and b is evaluated to be 0.5 Å in the point dipole approximation, which could be ascribed to the following: (1) the difference between the structures in the crystal form and in solution, (2) a small modification due to the cysteine to serine mutation, (3) differences of the species, and (4) the accuracy of the DFT calculation. As for DFT calculation, we did not consider the protein environment for simplification. Weber at al. have showed DFT calculation of flavin molecule including with local environment of protein for the study of DNA photolyase [25]. For the more precise fitting, DFT calculation including protein environment would be required. Conversely, the 'dark state' structure does not fit to the experimental result. Figure 3(b-e) shows the comparison with the different crystal structures[15, 18, 19]. The crystal structures in the dimer in the two dimers and in the 3 dimers did not fit to the PELDOR results, which is consistent with the point that aureochrome functions as a dimeric structure in the light state. Therefore, we concluded that our observed state is close to the 'light state' having the dimeric crystal structure in *P. tricornutum*[15]. Figure 4 shows the PELDOR signals (a) of LOV-C254S, and PZ-C254S (b) without DNA and (c) with DNA. All the PELDOR signals have the same oscillation pattern and frequency, indicating that there is no change observed so that the structure is identical.

The structural change between the 'dark state' and 'light state' is ascribed to the formation of the adduct between FMN and Cys254, which induces the flipping of Gln317 [26-28]. Our data suggest that LOV-C254S forms a dimer without the formation of a cysteinyl adduct in the radical state. It is consistent with a recent report that showed that the replacement of cysteine with alanine in Vivid-LOV still permitted the protein to dimerize and to conduct signals. Therefore, signal transfer is not dependent upon adduct formation but instead upon protonation of FMN in Vivid-LOV[29]. In addition, the similarity of the PELDOR signals between LOV-C254S and PZ-C254S with and without DNA, suggested that the LOV domains in PZ form a dimer with a similar conformation to that of the LOV dimer in the light state.

AUTHOR INFORMATION

Corresponding Authors
* mino@bio.phys.nagoya-u.ac.jp
* hisatomi@ess.sci.osaka-u.ac.jp

Present Address
$Hiroki Nagashima, Laser Molecular Photoscience Laboratory, Molecular Photoscience Research Center, Kobe University, 1-1 Rokkodaicho, Nada-ku, Kobe 657-8501, Japan.

Notes

The authors declare no competing financial interests.

ACKNOWLEDGMENT

This work was partly supported by Nanotechnology Platform Program (Molecule and Material Synthesis) of the Ministry of Education, Culture, Sports, Science and Technology (MEXT), Japan and by a Grant-in-Aid for Scientific Research (C) to O.H. (No. 26440077).

REFERENCES

[1] Takahashi, F. (2016) Blue-light-regulated transcription factor, Aureochrome, in photosynthetic stramenopiles, *J. Plant. Res. 129*, 189-197.

[2] Takahashi, F., Yamagata, D., Ishikawa, M., Fukamatsu, Y., Ogura, Y., Kasahara, M., Kiyosue, T., Kikuyama, M., Wada, M., and Kataoka, H. (2007) AUREOCHROME, a photoreceptor required for photomorphogenesis in stramenopiles, *Proc. Natl. Acad. Sci. U.S. A. 104*, 19625-19630.

[3] Vinson, C. R., Sigler, P. B., and McKnight, S. L. (1989) SCISSORS-GRIP MODEL FOR DNA RECOGNITION BY A

FAMILY OF LEUCINE ZIPPER PROTEINS, *Science 246*, 911-916.
[4] Vinson, C. R., Hai, T. W., and Boyd, S. M. (1993) DIMERIZATION SPECIFICITY OF THE LEUCINE ZIPPER-CONTAINING BZIP MOTIF ON DNA-BINDING - PREDICTION AND RATIONAL DESIGN, *Genes Dev. 7*, 1047-1058.
[5] Landschulz, W. H., Johnson, P. F., and McKnight, S. L. (1988) THE LEUCINE ZIPPER - A HYPOTHETICAL STRUCTURE COMMON TO A NEW CLASS OF DNA-BINDING PROTEINS, *Science 240*, 1759-1764.
[6] Fujii, Y., Shimizu, T., Toda, T., Yanagida, M., and Hakoshima, T. (2000) Structural basis for the diversity of DNA recognition by bZIP transcription factors, *Nat. Struct. Biol. 7*, 889-893.
[7] Schutze, K., Harter, K., and Chaban, C. (2008) Post-translational regulation of plant bZIP factors, *Trends. Plant Sci. 13*, 247-255.
[8] Alexandre, M. T. A., Domratcheva, T., Bonetti, C., van Wilderen, L. J. G. W., van Grondelle, R., Groot, M.-L., Hellingwerf, K. J., and Kennis, J. T. M. (2009) Primary Reactions of the LOV2 Domain of Phototropin Studied with Ultrafast Mid-infrared Spectroscopy and Quantum Chemistry, *Biophys. J. 97*, 227-237.
[9] Zoltowski, B. D., and Gardner, K. H. (2011) Tripping the Light Fantastic: Blue-Light Photoreceptors as Examples of Environmentally Modulated Protein-Protein Interactions, *Biochemistry 50*, 4-16.
[10] Salomon, M., Christie, J. M., Knieb, E., Lempert, U., and Briggs, W. R. (2000) Photochemical and mutational analysis of the FMN-binding domains of the plant blue light receptor, phototropin, *Biochemistry 39*, 9401-9410.
[11] Nakatani, Y., and Hisatomi, O. (2015) Molecular Mechanism of Photozipper, a Light-Regulated Dimerizing Module Consisting of the bZIP and LOV Domains of Aureochrome-1, *Biochemistry 54*, 3302-3313.
[12] Hisatomi, O., Takeuchi, K., Zikihara, K., Ookubo, Y., Nakatani, Y., Takahashi, F., Tokutomi, S., and Kataoka, H. (2013) Blue light-induced conformational changes in a light-regulated transcription factor, aureochrome-1, *Plant Cell Physiol. 54*, 93-106.
[13] Hisatomi, O., Nakatani, Y., Takeuchi, K., Takahashi, F., and Kataoka, H. (2014) Blue light-induced dimerization of monomeric aureochrome-1 enhances its affinity for the target sequence, *J. Biol. Chem. 289*, 17379-17391.
[14] Hisatomi, O., and Furuya, K. (2015) A light-regulated bZIP module, photozipper, induces the binding of fused proteins to the target DNA sequence in a blue light-dependent manner, *Photochem. Photobiol. Sci. 14*, 1998-2006.
[15] Heintz, U., and Schlichting, I. (2016) Blue light-induced LOV domain dimerization enhances the affinity of Aureochrome 1a for its target DNA sequence, *Elife 5*, e11860.
[16] Herman, E., Sachse, M., Kroth, P. G., and Kottke, T. (2013) Blue-light-induced unfolding of the Jalpha helix allows for the dimerization of aureochrome-LOV from the diatom Phaeodactylum tricornutum, *Biochemistry 52*, 3094-3101.
[17] Herman, E., and Kottke, T. (2015) Allosterically regulated unfolding of the A'alpha helix exposes the dimerization site of the blue-light-sensing aureochrome-LOV domain, *Biochemistry 54*, 1484-1492.
[18] Banerjee, A., Herman, E., Kottke, T., and Essen, L. O. (2016) Structure of a Native-like Aureochrome 1a LOV Domain Dimer from Phaeodactylum tricornutum, *Structure 24*, 171-178.
[19] Mitra, D., Yang, X., and Moffat, K. (2012) Crystal structures of Aureochrome1 LOV suggest new design strategies for optogenetics, *Structure 20*, 698-706.
[20] Asada, M., and Mino, H. (2015) Location of the High-Affinity Mn^{2+} Site in Photosystem II Detected by PELDOR, *J. Phys. Chem. B 119*, 10139-10144.
[21] Jeschke, G., Chechik, V., Ionita, P., Godt, A., Zimmermann, H., Banham, J., Timmel, C. R., Hilger, D., and Jung, H. (2006) DeerAnalysis2006 - a comprehensive software package for analyzing pulsed ELDOR data, *Appl. Magn. Reson. 30*, 473-498.
[22] Frisch, M. J., Trucks, G. W., Schlegel, H. B., Scuseria, G. E., Robb, M. A., Cheeseman, J. R., Scalmani, G., Barone, V., Petersson, G. A., Nakatsuji, H., Caricato, X. L., M. , Marenich, A., Bloino, J., Janesko, B. G., Gomperts, R., Mennucci, B., Hratchian, H. P., Ortiz, J. V., Izmaylov, A. F., Sonnenberg, J. L., Williams-Young, D., Ding, F., Lipparini, F., Egidi, F., Goings, J., Peng, B., Petrone, A., Henderson, T., Ranasinghe, D., Zakrzewski, V. G., Gao, J., Rega, N., Zheng, G., Liang, W., Hada, M., Ehara, M., Toyota, K., Fukuda, R., Hasegawa, J., Ishida, M., Nakajima, T., Honda, Y., Kitao, O., Nakai, H., Vreven, T., Throssell, K., Montgomery, J., J. A. , Peralta, J. E., Ogliaro, F., Bearpark, M., Heyd, J. J., Brothers, E., Kudin, K. N., Staroverov, V. N., Keith, T., Kobayashi, R., Normand, J., Raghavachari, K., Rendell, A., Burant, J. C., Iyengar, S. S., Tomasi, J., Cossi, M., Millam, J. M., Klene, M., Adamo, C., Cammi, R., Ochterski, J. W., Martin, R. L., Morokuma, K., Farkas, O., Foresman, J. B., and Fox, D. J. (2016) Gaussian 09, Revision D.01 ed., Gaussian, Inc., Wallingford CT.
[23] Kay, C. W., Schleicher, E., Kuppig, A., Hofner, H., Rudiger, W., Schleicher, M., Fischer, M., Bacher, A., Weber, S., and Richter, G. (2003) Blue light perception in plants. Detection and characterization of a light-induced neutral flavin radical in a C450A mutant of phototropin, *J. Biol. Chem. 278*, 10973-10982.
[24] Kay, C. W. M., Elsasser, C., Bittl, R., Farrell, S. R., and Thorpe, C. (2006) Determination of the distance between the two neutral flavin radicals in augmenter of liver regeneration by pulsed ELDOR, *J. Am. Chem. Soc. 128*, 76-77.
[25] Weber, S., Mobius, K., Richter, G., and Kay, C. W. M. (2001) The electronic structure of the flavin cofactor in DNA photolyase, *J. Am. Chem. Soc. 123*, 3790-3798.
[26] Crosson, S., and Moffat, K. (2002) Photoexcited structure of a plant photoreceptor domain reveals a light-driven molecular switch, *Plant Cell 14*, 1067-1075.
[27] Vaidya, A. T., Chen, C.-H., Dunlap, J. C., Loros, J. J., and Crane, B. R. (2011) Structure of a Light-Activated LOV Protein Dimer That Regulates Transcription, *Sci. Signal. 4*.
[28] Zoltowski, B. D., Schwerdtfeger, C., Widom, J., Loros, J. J., Bilwes, A. M., Dunlap, J. C., and Crane, B. R. (2007) Conformational switching in the fungal light sensor vivid, *Science 316*, 1054-1057.
[29] Yee, E. F., Diensthuber, R. P., Vaidya, A. T., Borbat, P. P., Engelhard, C., Freed, J. H., Bittl, R., Moglich, A., and Crane, B. R. (2015) Signal transduction in light-oxygen-voltage receptors lacking the adduct-forming cysteine residue, *Nat. Commun. 6*, 10079.